

# Trajectory-based data-driven predictive control and the state-space predictor

Levi D. Reyes Premer, Arash J. Khabbazi, and Kevin J. Kircher, *Member, IEEE*

**Abstract**—We define trajectory predictive control (TPC) as a family of output-feedback indirect data-driven predictive control (DDPC) methods that represent the output trajectory of a discrete-time system as a linear function of the recent input/output history and the planned input trajectory. This paper shows that for different choices of the trajectory predictor, TPC encompasses a wide variety of DDPC methods, including subspace predictive control (SPC), closed-loop SPC,  $\gamma$ -DDPC, causal- $\gamma$ -DDPC, transient predictive control, and others. This paper introduces a trajectory predictor that corresponds to a linear state-space model with the recent input/output history as the state. With this state-space predictor, TPC is a special case of linear model predictive control and therefore inherits its mature theory. In numerical experiments, TPC performance approaches the limit of oracle  $H_2$ -optimal control with perfect knowledge of the underlying system model. For TPC with small training datasets, the state-space predictor outperforms other predictors because it has fewer parameters.

**Index Terms**—Data-driven predictive control, identification for control, model predictive control, system identification

## I. INTRODUCTION

**M**ODEL predictive control (MPC) has been applied successfully for decades in several industries [1], but can be costly to implement due in part to its reliance on a model that predicts how a system will respond to planned control inputs. Data-driven predictive control (DDPC) emerged as an alternative to MPC around 1999 [2] and has recently seen a resurgence of research activity [3]. Broadly speaking, where MPC often uses physics-based models developed by domain experts, DDPC aims to optimize closed-loop performance given only a set of past input/output data. As gathering information-rich input/output data can be costly or risky, especially in safety-critical applications, DDPC methods should ideally work with small training datasets gathered in closed loop under a reliable if suboptimal feedback controller.

DDPC methods can be categorized as indirect or direct [4], [5]. Indirect DDPC methods identify a system model then embed it in control optimization. Direct DDPC methods, such as data-enabled predictive control (DeePC) [6], directly embed the training data in control optimization, bypassing system identification. DeePC is based on Willems' fundamental lemma of behavioral system theory [7], [8], which represents

The authors are with the School of Mechanical Engineering, Purdue University, 585 Purdue Mall, West Lafayette, Indiana, USA. [{lreyespr, arashjkh, kkirche}@purdue.edu](mailto:{lreyespr, arashjkh, kkirche}@purdue.edu)

future input/output trajectories as linear combinations of input/output trajectories from the training data. While DeePC performs well for deterministic linear systems, it can break down under uncertainty or nonlinearity. This observation has motivated researchers to modify DeePC with a variety of relaxations and regularizations aimed at improving robustness [9], [10], [11], [12], [13].

DeePC modifications have progressively blurred the boundary between indirect and direct DDPC. In [11], for example, Dörfler et al. show that two direct DDPC variants are convex relaxations of indirect DDPC, with regularization corresponding to implicit system identification. In [13], Breschi et al. show that adding a least-norm constraint effectively makes DeePC an indirect method. In [14], Chiuso et al. establish a DDPC separation principle for linear, time-invariant (LTI) systems with quadratic costs and no constraints. In this setting, separating identification from the rest of DDPC design does not reduce DDPC's closed-loop performance. Conducting system identification separately also has the advantage of providing an explicit model with quantified uncertainty, enabling principled analysis, simulation, and tuning of controllers [5].

This paper considers a family of indirect DDPC methods that we refer to as trajectory predictive control (TPC). While established system identification methods traditionally focus on learning an LTI state-space model [15], [16], TPC methods represent the full output trajectory over the prediction horizon as a linear function of the recent input/output history and the planned input trajectory. For different trajectory predictor structures, TPC encompasses a wide range of indirect DDPC methods that have recently been proposed. As the recent input/output history is perfectly observed, TPC enables output-feedback control without state estimation.

This paper introduces a trajectory predictor that, to the authors' knowledge, has not been studied in the DDPC literature. Unlike the trajectory predictors that have been studied to date, the predictor studied here corresponds to an LTI state-space model with the recent input/output history as the state. This correspondence establishes TPC with the 'state-space predictor' as a special case of conventional MPC with an LTI state-space model. TPC therefore inherits MPC's mature theory [17], such as conditions for stability [18] and recursive feasibility [19], and can be extended to a robust [20], stochastic [21], or scenario [22] framework using established methods. In numerical experiments, TPC with the state-space predictor performs as well as TPC with any other predictor, approaching the limit of an oracle linear-quadratic-Gaussian (LQG) controller that has perfect knowledge of the underlying system

model. For small training datasets, the state-space predictor outperforms other trajectory predictors because it has fewer parameters.

In summary, this paper makes three main contributions. First, it establishes TPC as a unifying framework for indirect DDPC. This paper shows how TPC encompasses a wide range of indirect DDPC variants and how TPC relates to direct DDPC via DeePC. Second, this paper introduces a trajectory predictor that makes TPC a special case of MPC with an LTI state-space model. Conceptually, this result brings DDPC full circle, returning it to the well-studied framework of MPC. Pragmatically, this result makes a mature body of LTI MPC theory, such as conditions for stability and recursive feasibility, applicable to DDPC. Third, this paper shows through numerical experiments that TPC with various predictors approaches the limit of oracle LQG control, even with small training datasets gathered in closed loop, and highlights the state-space predictor's data-efficiency.

The rest of this paper is organized as follows. §I-A collects notation and mathematical preliminaries. §II introduces the general TPC framework. §III surveys existing trajectory predictors, how to fit them, and how they relate TPC to existing DDPC variants. §IV introduces the state-space predictor, establishes its correspondence to an LTI state-space system, and compares it to other trajectory predictors. §V presents numerical experiments. §VI discusses limitations of this paper and possible directions for future work.

### A. Notation and preliminaries

The sets of real scalars, real  $n$ -dimensional column vectors, and real  $m \times n$  matrices are  $\mathbf{R}$ ,  $\mathbf{R}^n$ , and  $\mathbf{R}^{m \times n}$ , respectively. An identity matrix is  $I_n \in \mathbf{R}^{n \times n}$  and  $0_{m,n} \in \mathbf{R}^{m \times n}$  is a matrix of zeros. The stacked column vector with  $x \in \mathbf{R}^n$  above  $y \in \mathbf{R}^m$  is

$$(x, y) \text{ or } \begin{bmatrix} x \\ y \end{bmatrix} \in \mathbf{R}^{n+m}.$$

The Moore-Penrose pseudoinverse of  $A \in \mathbf{R}^{m \times n}$  with  $\text{rank}(A) = m \leq n$  is  $A^\dagger := A^\top (AA^\top)^{-1} \in \mathbf{R}^{n \times m}$ , where  $:=$  denotes a definition. For  $A \in \mathbf{R}^{m \times n}$  with  $\text{rank}(A) = m \leq n$  and  $b \in \mathbf{R}^m$ ,  $\hat{x} = A^\dagger b$  is the unique minimizer over  $x$  of  $\|x\|_2$  subject to  $Ax = b$ , where  $\|\cdot\|_2$  is the Euclidean norm. For the linear model  $Y = \Theta X + E$  with targets  $Y \in \mathbf{R}^{m \times n}$ , parameters  $\Theta \in \mathbf{R}^{m \times p}$ , features  $X \in \mathbf{R}^{p \times n}$ , errors  $E \in \mathbf{R}^{m \times n}$ , and  $\text{rank}(X) = p \leq n$ ,  $\hat{\Theta} = YX^\dagger$  is the unique minimizer over  $\Theta$  of the mean squared error

$$\|Y - \Theta X\|_{\text{Fro}}^2 / n := \text{trace}((Y - \Theta X)^\top (Y - \Theta X)) / n,$$

where  $\|\cdot\|_{\text{Fro}}$  is the Frobenius norm.

## II. TRAJECTORY PREDICTIVE CONTROL

We consider a system with discrete time index  $t$ . At each  $t$ , the controller sends an input  $u(t) \in \mathbf{R}^{n_u}$  to the system, the system evolves to a new state (through unknown dynamics, possibly influenced by unmeasured disturbances), and the controller receives a (possibly noisy) output  $y(t) \in \mathbf{R}^{n_y}$  from the system. We define TPC, summarized in Algorithm 1, as

---

### Algorithm 1 Trajectory predictive control

---

**Input:** Trajectory predictor matrices  $P$  and  $F$ ; cost and constraint functions  $c_0, \dots, c_J$ ; regularizer  $r$ ; initial input/output history  $z_p(1)$

**for**  $t = 1, 2, \dots$

- Solve (2) and implement  $u(t) = u^*(1|t)$
- Observe  $y(t)$  and form

$$z(t) = \begin{bmatrix} u(t) \\ y(t) \end{bmatrix}, \quad z_p(t+1) = \begin{bmatrix} z(t-m+1) \\ \vdots \\ z(t) \end{bmatrix}$$

**end for**

---

a family of output-feedback indirect DDPC algorithms that choose the input  $u(t)$  based on the last  $m$  inputs and outputs,

$$z_p(t) = \begin{bmatrix} z(t-m) \\ \vdots \\ z(t-1) \end{bmatrix}, \quad \text{where } z(t) = \begin{bmatrix} u(t) \\ y(t) \end{bmatrix} \in \mathbf{R}^{n_z} \quad (1)$$

and  $n_z = n_u + n_y$ , to

$$\begin{aligned} & \text{minimize} \quad c_0(u_f(t), y_f(t)) + r(e_f(t)) \\ & \text{subject to} \quad c_j(u_f(t), y_f(t)) \leq 0, \quad j = 1, \dots, J \\ & \quad y_f(t) = Pz_p(t) + Fu_f(t) + e_f(t). \end{aligned} \quad (2)$$

The variables in (2) are the planned input and output trajectories  $u_f(t) \in \mathbf{R}^{hn_u}$  and  $y_f(t) \in \mathbf{R}^{hn_y}$ , where  $h$  is the prediction horizon, and  $e_f(t) \in \mathbf{R}^{hn_y}$ . Depending on the context,  $e_f(t)$  can be viewed as a slack variable, as noise, or as a prediction or estimation error. We write the variables as

$$u_f(t) = \begin{bmatrix} u(1|t) \\ \vdots \\ u(h|t) \end{bmatrix}, \quad y_f(t) = \begin{bmatrix} y(1|t) \\ \vdots \\ y(h|t) \end{bmatrix}, \quad e_f(t) = \begin{bmatrix} e(1|t) \\ \vdots \\ e(h|t) \end{bmatrix},$$

where the notation  $i|t$  indicates a plan or prediction made  $i$  steps ahead at time  $t$ . For example,  $u(1|t)$  is the plan for  $u(t)$  made at time  $t$ . If the cost and constraint functions  $c_0, \dots, c_J : \mathbf{R}^{hn_u} \times \mathbf{R}^{hn_y} \rightarrow \mathbf{R}$  and the regularizer  $r : \mathbf{R}^{hn_y} \rightarrow \mathbf{R} \cup \{\infty\}$  are convex, then (2) is a convex optimization problem.

This paper focuses on the general trajectory predictor

$$y_f(t) = Pz_p(t) + Fu_f(t) + e_f(t). \quad (3)$$

We assume that  $P \in \mathbf{R}^{hn_y \times mn_z}$  and  $F \in \mathbf{R}^{hn_y \times hn_u}$  are identified from a trajectory  $\tilde{z}(1), \dots, \tilde{z}(d)$  of input/output examples from the system, with  $e_f(t)$  treated as an estimation error to be minimized. We organize the training data (denoted by tildes) into Hankel matrices containing  $n = d - m - h + 1$  trajectory examples:

$$\begin{aligned} \tilde{Z} &= [\tilde{z}_p(m+1) \quad \dots \quad \tilde{z}_p(d-h+1)] \in \mathbf{R}^{mn_z \times n} \\ \tilde{U} &= [\tilde{u}_f(m+1) \quad \dots \quad \tilde{u}_f(d-h+1)] \in \mathbf{R}^{hn_u \times n} \\ \tilde{Y} &= [\tilde{y}_f(m+1) \quad \dots \quad \tilde{y}_f(d-h+1)] \in \mathbf{R}^{hn_y \times n}, \end{aligned}$$

where

$$\tilde{u}_f(t) = \begin{bmatrix} \tilde{u}(t) \\ \vdots \\ \tilde{u}(t+h-1) \end{bmatrix}, \quad \tilde{y}_f(t) = \begin{bmatrix} \tilde{y}(t) \\ \vdots \\ \tilde{y}(t+h-1) \end{bmatrix},$$

and  $\tilde{z}_p(t)$  is defined as in (1).

Most of this paper will take the regularizer to be

$$r(e_f(t)) = \delta_0(e_f(t)) = \begin{cases} 0 & \text{if } e_f(t) = 0 \\ \infty & \text{otherwise.} \end{cases}$$

With  $r = \delta_0$ , the general TPC problem (2) is only feasible if  $e_f(t) = 0$ , so an equivalent problem is to

$$\begin{aligned} & \text{minimize } c_0(u_f(t), y_f(t)) \\ & \text{subject to } c_j(u_f(t), y_f(t)) \leq 0, \quad j = 1, \dots, J \\ & \quad y_f(t) = Pz_p(t) + Fu_f(t), \end{aligned} \quad (4)$$

with variables  $u_f(t)$ ,  $y_f(t)$ . Less strict regularizers, such as

$$r(e_f(t)) = \lambda \|e_f(t)\|_1 \text{ or } r(e_f(t)) = \lambda \|e_f(t)\|_2^2,$$

let the optimization steer the planned trajectory  $u_f(t)$ ,  $y_f(t)$  away from the central prediction  $u_f(t)$ ,  $Pz_p(t) + Fu_f(t)$  to reduce the cost  $c_0(u_f(t), y_f(t))$ , a tactic that several recent DDPC variants use. Smaller values of the tunable scalar hyperparameter  $\lambda > 0$  allow larger deviations. As  $\lambda \rightarrow \infty$ , the norm regularizers approach  $\delta_0$ .

DDPC research often restricts the cost to be quadratic and the constraints to be separable in the input and output. The formulation (2) does not make those restrictions in general but includes them as special cases.

The memory  $m$  and prediction horizon  $h$  are key determinants of TPC performance. Tuning  $m$  and  $h$  typically involves specifying an initial  $h$  (possibly based on an estimate of the open-loop system's dominant time constant), selecting a corresponding  $m$  (through cross-validation or another model selection procedure) such that the predictor generalizes well to test data, testing TPC in Monte Carlo simulation with the tuned model and randomization consistent with predictor uncertainty, repeating the above until TPC performs well in simulation, then deploying on the real system and adjusting if needed.

### III. DDPC AND TRAJECTORY PREDICTORS

Motivations for the predictor structure (3) in the TPC problem (2) are twofold. First, the predictor's linearity ensures that if  $c_0, \dots, c_J$  and  $r$  are convex, then the TPC problem (2) is convex and can typically be solved efficiently and globally by off-the-shelf software [23]. Second, the predictor structure aligns with Willems' fundamental lemma of behavioral system theory [7], [8], a foundation of DDPC.

Willems' fundamental lemma applies if the underlying system is deterministic, LTI, and controllable, and if the training inputs  $\tilde{u}(1), \dots, \tilde{u}(d)$  are persistently exciting [24], [25]. Given the recent input/output history  $z_p(t)$ , Willems' fundamental lemma implies that  $u_f(t), y_f(t)$  is a possible system trajectory if and only if there exists an  $\alpha(t) \in \mathbf{R}^n$  such that

$$\begin{bmatrix} \tilde{Z} \\ \tilde{U} \\ \tilde{Y} \end{bmatrix} \alpha(t) = \begin{bmatrix} z_p(t) \\ u_f(t) \\ y_f(t) \end{bmatrix}. \quad (5)$$

For fixed  $z_p(t)$  and  $u_f(t)$ , (5) implies that  $y_f(t) = \tilde{Y}\alpha(t)$  is a possible output trajectory for any  $\alpha(t)$  satisfying

$$\begin{bmatrix} \tilde{Z} \\ \tilde{U} \end{bmatrix} \alpha(t) = \begin{bmatrix} z_p(t) \\ u_f(t) \end{bmatrix}. \quad (6)$$

The dimension  $n$  of  $\alpha(t)$  may exceed the row rank of  $[\tilde{Z}^\top \quad \tilde{U}^\top]^\top$ , which is  $mn_z + hn_u$  under persistent excitation [24], [25], so a solution  $\alpha(t)$  to (6) may not be unique.

The DeePC method [6] replaces the trajectory predictor (3) in problem (4) by (5), choosing  $u_f(t)$ ,  $y_f(t)$ ,  $\alpha(t)$  to

$$\begin{aligned} & \text{minimize } c_0(u_f(t), y_f(t)) \\ & \text{subject to } c_j(u_f(t), y_f(t)) \leq 0, \quad j = 1, \dots, J \\ & \quad \begin{bmatrix} \tilde{Z} \\ \tilde{U} \\ \tilde{Y} \end{bmatrix} \alpha(t) = \begin{bmatrix} z_p(t) \\ u_f(t) \\ y_f(t) \end{bmatrix}. \end{aligned} \quad (7)$$

DeePC performs well for deterministic LTI systems, but under uncertainty or nonlinearity, the true system behavior can diverge wildly from the planned trajectory  $u_f^*(t)$ ,  $y_f^*(t)$  corresponding to an optimal  $\alpha^*(t)$ . In [26], Moffat et al. explain this divergence in part through the notion of *optimism bias*: When many  $\alpha(t)$  may satisfy (5), the DeePC optimization is free to choose an  $\alpha^*(t)$  that reduces the cost  $c_0$ . DeePC also suffers from bias when training data are gathered in closed loop [27], [26]. DeePC's sensitivity to uncertainty and nonlinearity has motivated modifications that improve robustness by regularizing  $\alpha(t)$  or by introducing and regularizing slack variables [28], [10], [11], [13].

#### A. DeePC, SPC, $\gamma$ -DDPC, and the subspace predictor

Connections between (5) and (3) can be seen by finding the least-norm  $\hat{\alpha}(t)$  satisfying (6), which solves

$$\begin{aligned} & \text{minimize } \|\alpha(t)\|_2 \\ & \text{subject to } \begin{bmatrix} \tilde{Z} \\ \tilde{U} \end{bmatrix} \alpha(t) = \begin{bmatrix} z_p(t) \\ u_f(t) \end{bmatrix}. \end{aligned}$$

If  $[\tilde{Z}^\top \quad \tilde{U}^\top]^\top$  has full row rank, then

$$\hat{\alpha}(t) = \begin{bmatrix} \tilde{Z} \\ \tilde{U} \end{bmatrix}^\dagger \begin{bmatrix} z_p(t) \\ u_f(t) \end{bmatrix}.$$

The output trajectory corresponding to  $\hat{\alpha}(t)$  is

$$\hat{y}_f(t) = \tilde{Y}\hat{\alpha}(t) = P_{\text{sbs}}z_p(t) + F_{\text{sbs}}u_f(t)$$

with

$$[P_{\text{sbs}} \quad F_{\text{sbs}}] = \tilde{Y} \begin{bmatrix} \tilde{Z} \\ \tilde{U} \end{bmatrix}^\dagger. \quad (8)$$

The trajectory predictor (3) with  $P = P_{\text{sbs}}$  and  $F = F_{\text{sbs}}$  from (8) is known as the *subspace predictor* [26], [2], [29]. TPC with the subspace predictor and  $r = \delta_0$  is known as subspace predictive control (SPC) [2]. SPC is equivalent to DeePC augmented with the constraint  $\alpha(t) = \hat{\alpha}(t)$ , the least-norm solution to (6) [30].

The subspace predictor matrices  $P_{\text{sbs}}$  and  $F_{\text{sbs}}$  also solve a least squares estimation problem. To see this, we form an example of the trajectory predictor (3) at each  $t = m+1, \dots, d-h+1$ . Horizontally concatenating the examples gives

$$\tilde{Y} = P\tilde{Z} + F\tilde{U} + \tilde{E},$$

where  $\tilde{E} = [\tilde{e}_f(m+1) \quad \dots \quad \tilde{e}_f(d-h+1)] \in \mathbf{R}^{hn_y \times n}$  and the  $\tilde{e}_f(t)$  are viewed as estimation errors. The subspace

predictor (8) therefore minimizes the mean squared error  $\|\tilde{Y} - P\tilde{Z} - F\tilde{U}\|_{\text{Fro}}^2/n$ .

In [13], Breschi et al. obtain an explicit formula for the subspace predictor from the LQ decomposition

$$\begin{bmatrix} \tilde{Z} \\ \tilde{U} \\ \tilde{Y} \end{bmatrix} = \begin{bmatrix} L_{11} & & \\ L_{21} & L_{22} & \\ L_{31} & L_{32} & L_{33} \end{bmatrix} \begin{bmatrix} Q_1 \\ Q_2 \\ Q_3 \end{bmatrix}. \quad (9)$$

Here  $L_{11} \in \mathbf{R}^{mn_z \times mn_z}$ ,  $L_{22} \in \mathbf{R}^{hn_u \times hn_u}$ , and  $L_{33} \in \mathbf{R}^{hn_y \times hn_y}$  are lower triangular;  $L_{21} \in \mathbf{R}^{hn_u \times mn_z}$ ,  $L_{31} \in \mathbf{R}^{hn_y \times mn_z}$ , and  $L_{32} \in \mathbf{R}^{hn_y \times hn_u}$  are generally dense; and  $Q_1 \in \mathbf{R}^{mn_z \times n}$ ,  $Q_2 \in \mathbf{R}^{hn_u \times n}$ , and  $Q_3 \in \mathbf{R}^{hn_y \times hn_y}$  are orthonormal: Each  $Q_i Q_j^\top$  equals an identity matrix if  $i = j$  and a zero matrix if  $i \neq j$ . If  $[\tilde{Z}^\top \quad \tilde{U}^\top]^\top$  has full row rank, then  $L_{11}$  and  $L_{22}$  are invertible and

$$\begin{aligned} [P_{\text{sbs}} \quad F_{\text{sbs}}] &= \tilde{Y} [Q_1^\top \quad Q_2^\top] \begin{bmatrix} L_{11} & \\ L_{21} & L_{22} \end{bmatrix}^{-1} \\ &= \tilde{Y} [Q_1^\top \quad Q_2^\top] \begin{bmatrix} L_{11}^{-1} \\ -L_{22}^{-1} L_{21} L_{11}^{-1} & L_{22}^{-1} \end{bmatrix}, \end{aligned} \quad (10)$$

with the second line from proposition 3.9.7 of [31]. But

$$\tilde{Y} [Q_1^\top \quad Q_2^\top] = [L_{31} \quad L_{32}]$$

by (9) and orthonormality of the  $Q_i$ , so

$$F_{\text{sbs}} = L_{32} L_{22}^{-1}, \quad P_{\text{sbs}} = (L_{31} - F_{\text{sbs}} L_{21}) L_{11}^{-1}. \quad (11)$$

TPC with the subspace predictor in the form (11) is known as  $\gamma$ -DDPC [13]. In [30], Sader et al. define regularized- $\gamma$ -DDPC by adding a slack variable equivalent to  $e_f(t)$  and regularizing it with  $r(e_f(t)) = \lambda \|e_f(t)\|_2^2$ .

### B. Causal- $\gamma$ -DDPC and the multistep predictor

In general, the subspace predictor is not causal: It models future inputs as influencing past outputs. To see this, we write  $F$  in the general trajectory predictor (3) in block form as

$$F = \begin{bmatrix} F_{11} & \cdots & F_{1h} \\ \vdots & \ddots & \vdots \\ F_{h1} & \cdots & F_{hh} \end{bmatrix} \quad \text{where } F_{ij} \in \mathbf{R}^{n_y \times n_u}.$$

**Definition 1.** The trajectory predictor (3) is **causal** if  $F$  is block lower triangular (BLT):  $F_{ij} = 0$  for  $i = 1, \dots, h-1$  and  $j = i+1, \dots, h$ .

Causality implies that the planned input  $u(j|t)$  in (2) can only influence the planned output  $y(i|t)$  if  $i \geq j$ . Although  $L_{22}^{-1}$  is lower triangular,  $L_{32}$  is dense in general. In the subspace predictor,  $F_{\text{sbs}}$  is the product of the dense matrix  $L_{32}$  and the lower triangular matrix  $L_{22}^{-1}$ , so in general  $F_{\text{sbs}}$  is dense and the subspace predictor is not causal.

In [30], Sader et al. investigate the *multistep predictor*  $P_{\text{mlt}}$ ,  $F_{\text{mlt}}$ , defined as solving the constrained least squares problem

$$\text{minimize } \|\tilde{Y} - P\tilde{Z} - F\tilde{U}\|_{\text{Fro}}^2$$

subject to  $F$  BLT

with variables  $P$  and  $F$ . Sader et al. show (up to calculation of the block inverse in (10)) that

$$F_{\text{mlt}} = \text{BLT}(L_{32}) L_{22}^{-1}, \quad P_{\text{mlt}} = (L_{31} - F_{\text{mlt}} L_{21}) L_{11}^{-1}. \quad (12)$$

In (12), the operator  $\text{BLT}(L_{32})$  zeros out the strictly block upper triangular part of  $L_{32}$ , returning a version of  $L_{32}$  that is BLT but otherwise unchanged. Comparing (12) to (11) shows that the multistep predictor can be viewed as a ‘causalized’ version of the subspace predictor.

In [30], Sader et al. refer to TPC with the multistep predictor (12) and  $r = \delta_0$  as causal- $\gamma$ -DDPC. In numerical examples, causal- $\gamma$ -DDPC outperforms  $\gamma$ -DDPC and SPC, particularly for small training datasets gathered in closed loop. In numerical examples, adding the slack variable  $e_f(t)$  with  $r(e_f(t)) = \lambda \|e_f(t)\|_2^2$ , a variant that Sader et al. call regularized-causal- $\gamma$ -DDPC, improves closed-loop performance, with larger improvements for smaller datasets.

### C. Transient predictive control and the transient predictor

In [29], [26], Moffat et al. develop another approach to estimating the multistep predictor. They define the *transient predictor* in terms of matrices  $\Phi^p \in \mathbf{R}^{hn_y \times mn_z}$ ,  $\Phi^u \in \mathbf{R}^{hn_y \times mn_u}$ ,  $\Phi^y \in \mathbf{R}^{hn_y \times hn_y}$  satisfying

$$y_f(t) = \Phi^p z_p(t) + \Phi^u u_f(t) + \Phi^y y_f(t) + \varepsilon_f(t), \quad (13)$$

where  $\varepsilon_f(t) \in \mathbf{R}^{hn_y}$  is an error. To enforce causality, Moffat et al. require  $\Phi^u$  to be BLT and  $\Phi^y$  to be strictly BLT (meaning  $\Phi^y$  is BLT and  $\Phi_{11}^y = \dots = \Phi_{hh}^y = 0_{n_y, n_y}$ ). Rearranging (13) gives an instance of the trajectory predictor (3) with

$$\begin{aligned} P &= (I - \Phi^y)^{-1} \Phi^p, \quad F = (I - \Phi^y)^{-1} \Phi^u \\ e_f(t) &= (I - \Phi^y)^{-1} \varepsilon_f(t). \end{aligned} \quad (14)$$

The inverse in (14) exists because  $I - \Phi^y$  is lower triangular with ones along its diagonal.

In [29], Moffat et al. form the transient predictor  $P_{\text{trn}}$ ,  $F_{\text{trn}}$  from (14) with  $\Phi^p$ ,  $\Phi^u$ , and  $\Phi^y$  estimated from the LQ decomposition of the full Hankel matrix of input/output data. Alternatively, each  $i$ -step-ahead predictor can be estimated separately. For  $i = 1$ , the prediction of  $y(t)$  is  $\Phi_1^p z_p(t) + \Phi_{11}^u u(t)$ , where  $\Phi_i^p \in \mathbf{R}^{n_y \times mn_p}$  is the  $i$ th block row of  $\Phi^p$  and  $\Phi_{ij}^u \in \mathbf{R}^{n_y \times n_u}$  is the  $i, j$  block of  $\Phi^u$ . Horizontally concatenating the one-step-ahead examples for each  $t$  gives  $\tilde{Y}_1 \approx \Phi_1^p \tilde{Z} + \Phi_{11}^u \tilde{U}_1$ , where  $\tilde{Y}_1 \in \mathbf{R}^{n_y \times n}$  and  $\tilde{U}_1 \in \mathbf{R}^{n_u \times n}$  are the first block rows of  $\tilde{Y}$  and  $\tilde{U}$ . If  $[\tilde{Z}^\top \quad \tilde{U}_1^\top]^\top$  has full row rank, then the least squares estimate is

$$[\hat{\Phi}_1^p \quad \hat{\Phi}_{11}^u] = \tilde{Y}_1 \begin{bmatrix} \tilde{Z} \\ \tilde{U}_1 \end{bmatrix}^\dagger. \quad (15)$$

For  $i > 1$ , the  $i$ -step-ahead prediction of  $y(t+i-1)$  is

$$\begin{aligned} \Phi_i^p z_p(t) \\ + \Phi_{i,1:i}^u \begin{bmatrix} u(t) \\ \vdots \\ u(t+i-1) \end{bmatrix} + \Phi_{i,1:i-1}^y \begin{bmatrix} y(t) \\ \vdots \\ y(t+i-2) \end{bmatrix}, \end{aligned}$$

where  $\Phi_{i,1:i}^u = [\Phi_{i1}^u \cdots \Phi_{ii}^u]$  and  $\Phi_{i,1:i-1}^y = [\Phi_{i1}^y \cdots \Phi_{i,i-1}^y]$ . Horizontally concatenating the  $i$ -step-ahead examples gives  $\tilde{Y}_i \approx \Phi_i^p \tilde{Z} + \Phi_i^u \tilde{U}_{1:i} + \Phi_i^y \tilde{Y}_{1:i-1}$ , where  $\tilde{Y}_i \in \mathbf{R}^{n_y \times n}$  is the  $i$ th block row of  $\tilde{Y}$ ,  $\tilde{U}_{1:i} \in \mathbf{R}^{n_u \times n}$  contains block rows 1, ...,  $i$  of  $\tilde{U}$ , and  $\tilde{Y}_{1:i-1} \in \mathbf{R}^{(i-1)n_y \times n}$

contains block rows  $1, \dots, i-1$  of  $\tilde{Y}$ . If  $[\tilde{Z}^\top \quad \tilde{U}_{1:i}^\top \quad \tilde{Y}_{1:i-1}^\top]^\top$  has full row rank, then

$$[\hat{\Phi}_i^p \quad \hat{\Phi}_i^u \quad \hat{\Phi}_i^y] = \tilde{Y}_i \begin{bmatrix} \tilde{Z} \\ \tilde{U}_{1:i} \\ \tilde{Y}_{1:i-1} \end{bmatrix}^\dagger.$$

In [26], Moffat et al. refer to TPC with  $r = \delta_0$  and the predictor (14) as transient predictive control. They show that transient predictive control is not subject to optimism bias or to the bias that TPC with the subspace predictor suffers when training data are gathered in closed loop.

#### D. Closed-loop SPC and the fixed-length predictor

Dong et al. [32] and Chiuso et al. [14] form the *fixed-length predictor* as a structured special case of (13):

$$\Phi^p = \begin{bmatrix} \phi_1^p & \phi_2^p & \cdots & \phi_m^p \\ \phi_1^p & \cdots & \phi_{m-1}^p \\ \ddots & \ddots & \ddots & \ddots \end{bmatrix}, \quad \Phi^u = \begin{bmatrix} \phi_1^u & & & \\ \vdots & \ddots & & \\ \phi_h^u & \cdots & \phi_1^u & \end{bmatrix},$$

with blocks  $\phi_1^p, \dots, \phi_m^p \in \mathbf{R}^{n_y \times n_z}$ ,  $\phi_1^u, \dots, \phi_h^u \in \mathbf{R}^{n_y \times n_u}$ , and  $\phi_1^y, \dots, \phi_{h-1}^y \in \mathbf{R}^{n_y \times n_y}$ . The matrix  $\Phi^y$  is structured similarly to  $\Phi^u$  but strictly BLT. The (block)  $h \times m$  matrix  $\Phi^p$  may be wide, square, or tall. In any case, all elements below the  $\phi_1^p$  block diagonal are zero.

The fixed-length predictor can be fit sequentially, beginning by fitting the one-step-ahead model

$$y(t) \approx [\phi_1^p \quad \cdots \quad \phi_m^p] z_p(t) + \phi_1^u u(t)$$

for  $\phi_1^p, \dots, \phi_m^p, \phi_1^u$ . We then fit the two-step-ahead residual

$$\begin{aligned} y(t+1) - [0_{n_y, n_z} \quad \phi_1^p \quad \cdots \quad \phi_{m-1}^p] z_p(t) - \phi_1^u u(t+1) \\ \approx \phi_2^u u(t) + \phi_1^y y(t) \end{aligned}$$

for  $\phi_2^u$  and  $\phi_1^y$ . The residual fits proceed for each  $i$ -step-ahead predictor, subtracting the influence of all previously estimated parameters from  $y(t+i-1)$ . The residual fits end at  $i=h$  with estimation of  $\phi_h^u$  and  $\phi_{h-1}^y$ . The full  $\Phi^p$ ,  $\Phi^u$ , and  $\Phi^y$  can then be formed and the fixed-length predictor matrices  $P_{\text{fix}}$ ,  $F_{\text{fix}}$  defined as in (14).

In [32], Dong et al. refer to TPC with the fixed-length predictor and  $r = \delta_0$  as closed-loop SPC. They show that unlike the subspace predictor, the fixed-length predictor works with training data gathered in closed loop. In [14], Chiuso et al. use the fixed-length predictor to derive a separation principle for DDPC when the cost is the sum of quadratic penalties on  $u_f(t)$  and  $y_f(t)$ , there are no constraints, and the training data come from an underlying LTI stochastic system. The separation principle implies that in this setting, there is no loss of optimality from separating predictor identification from the rest of DDPC design.

In [33], Liu and Jansson use a predictor (introduced in [34]) with  $\Phi^u$  and  $\Phi^y$  structured as in the fixed-length predictor, but with  $\Phi^p$  either unstructured (as in the transient predictor) or constrained to have low rank. Liu and Jansson first fit a high-order autoregressive-with-exogenous-inputs (ARX) vector time series model to construct  $\Phi^u$  and  $\Phi^y$ , then fit the residual  $y_f(t) - \Phi^u u_f(t) - \Phi^y y_f(t) = \Phi^p z_p(t) + \varepsilon_f(t)$  for  $\Phi^p$  via least squares, optionally with a low-rank constraint that they satisfy using the singular value decomposition.

#### IV. MPC AND THE STATE-SPACE PREDICTOR

We define the *state-space predictor* such that the trajectory predictor (3) is equivalent to the LTI state-space model

$$\begin{aligned} z_p(t+1) &= Az_p(t) + Bu(t) + K\varepsilon(t) \\ y(t) &= Cz_p(t) + Du(t) + \varepsilon(t) \end{aligned} \quad (16)$$

for appropriate choices of  $A \in \mathbf{R}^{mn_z \times mn_z}$ ,  $B \in \mathbf{R}^{mn_z \times n_u}$ ,  $C \in \mathbf{R}^{hn_y \times mn_z}$ ,  $D \in \mathbf{R}^{hn_y \times hn_u}$ ,  $K \in \mathbf{R}^{mn_z \times n_y}$ , and  $\varepsilon(t) \in \mathbf{R}^{n_y}$ . We begin with the following observation.

**Proposition 1.** *For any causal trajectory predictor of the form (3), the one-step predictor (meaning the first  $n_y$ -block row of (3)) is a linear ARX model with autoregressive memory  $m$ , exogenous memory  $m+1$ , and delay zero.*

*Proof.* By definition 1,  $F_{12} = \cdots = F_{1m} = 0$  for any causal trajectory predictor (3), so the one-step-ahead predictor is

$$y(t) = P_1 z_p(t) + F_{11} u(t) + e(t). \quad (17)$$

The first block row of  $P$ ,  $P_1 \in \mathbf{R}^{n_y \times mn_z}$ , can be written as

$$P_1 = [P_{11}^u \quad P_{11}^y \quad \cdots \quad P_{1m}^u \quad P_{1m}^y]$$

with  $P_{1j}^u \in \mathbf{R}^{n_y \times n_u}$  and  $P_{1j}^y \in \mathbf{R}^{n_y \times n_y}$ . Recalling (1), expanding  $P_1$  and  $z_p(t)$  in (17) gives

$$\begin{aligned} y(t) - P_{11}^y y(t-m) - \cdots - P_{1m}^y y(t-1) \\ = P_{11}^u u(t-m) + \cdots + P_{1m}^u u(t-1) + F_{11} u(t) + e(t). \end{aligned}$$

This is a linear ARX( $m, m+1, 0$ ) model.  $\blacksquare$

In light of Proposition 1, we construct  $A$ ,  $B$ ,  $C$ ,  $D$ ,  $K$ , and  $\varepsilon_f(t) = (\varepsilon(t), \dots, \varepsilon(t+h-1)) \in \mathbf{R}^{hn_y}$  such that the trajectory predictor (3) is consistent with iteratively applying the one-step-ahead ARX model. Lemma 2 provides suitable definitions of the system matrices.

**Lemma 2.** *Let  $\varepsilon(t) = e(t)$ ,*

$$\begin{aligned} C &= P_1, \quad D = F_{11} \\ A &= \begin{bmatrix} 0_{(m-1)n_z, n_z} & I_{(m-1)n_z} \\ 0_{n_u, mn_z} & C \\ & \ddots \end{bmatrix} \\ B &= \begin{bmatrix} 0_{(m-1)n_z, n_u} \\ I_{n_u} \\ D \end{bmatrix}, \quad K = \begin{bmatrix} 0_{(m-1)n_z + n_u, n_y} \\ I_{n_y} \end{bmatrix}. \end{aligned} \quad (18)$$

*Then  $z_p(t)$ ,  $u(t)$ , and  $y(t)$  satisfy the causal one-step predictor (17) if and only if they satisfy the state-space model (16).*

*Proof.* With the definitions of  $C$ ,  $D$ , and  $\varepsilon(t)$ , the one-step predictor (17) is equivalent to the output equation in (16). For the dynamics, the definition (1) of  $z_p(t)$  implies that

$$\begin{aligned} z_p(t+1) &= \begin{bmatrix} z(t-m+1) \\ \vdots \\ z(t) \end{bmatrix} = \begin{bmatrix} 0_{(m-1)n_z, n_z} \\ I_{n_z} \end{bmatrix} z(t) \\ &+ \begin{bmatrix} 0_{(m-1)n_z, n_z} & I_{(m-1)n_z} \\ 0_{n_z} & 0_{n_z, (m-1)n_z} \end{bmatrix} z_p(t). \end{aligned} \quad (19)$$

Since  $z(t) = (u(t), y(t))$  and  $y(t) = Cz_p(t) + Du(t) + \varepsilon(t)$ ,

$$z(t) = \begin{bmatrix} I_{n_u} \\ 0_{n_y, n_u} \end{bmatrix} u(t) + \begin{bmatrix} 0_{n_u, n_y} \\ I_{n_y} \end{bmatrix} (Cz_p(t) + Du(t) + \varepsilon(t)).$$

---

**Algorithm 2** State-space predictor identification

---

**Input:** Memory  $m$ ; prediction horizon  $h$ ; training data matrices  $\tilde{Z}, \tilde{U}_1, \tilde{Y}_1$

- One-step-ahead fit:  $[C \quad D] = \tilde{Y}_1 \begin{bmatrix} \tilde{Z} \\ \tilde{U}_1 \end{bmatrix}^\dagger$
- $A, B, K$  from (18)
- $\mathcal{A} = A - KC, \mathcal{B} = B - KD$
- $\Phi^p, \Phi^u, \Phi^y$  from (22)
- Return  $P, F$  from (14)

---

Substituting this expression into (19) gives  $z_p(t+1) = Az_p(t) + Bu(t) + K\varepsilon(t)$  with the  $A, B$ , and  $K$  in (18).  $\blacksquare$

Lemma 2 establishes a correspondence between the state-space model (16) and the one-step-ahead predictor (17). To build the full state-space predictor in the form (3), we iteratively apply (16). Solving the output equation for  $\varepsilon(t)$  and substituting it into the dynamics gives

$$z_p(t+1) = \mathcal{A}z_p(t) + \mathcal{B}u(t) + Ky(t), \quad (20)$$

where  $\mathcal{A} = A - KC$  and  $\mathcal{B} = B - KD$ . For  $i > 0$ , iteratively applying this innovations-form model gives

$$\begin{aligned} y(t+i) &= C\mathcal{A}^i z_p(t) + Du(t+i) + \varepsilon(t+i) \\ &+ C \sum_{j=0}^{i-1} \mathcal{A}^{i-j-1} (\mathcal{B}u(t+j) + Ky(t+j)). \end{aligned} \quad (21)$$

Forming this model at each  $i = 1, \dots, h-1$  gives a predictor of the form (13) with

$$\begin{aligned} \Phi^p &= \begin{bmatrix} C\mathcal{A}^0 \\ \vdots \\ C\mathcal{A}^{h-1} \end{bmatrix}, \quad \Phi^u = \begin{bmatrix} D \\ C\mathcal{A}^0\mathcal{B} & D \\ \vdots & \ddots & \ddots \\ C\mathcal{A}^{h-2}\mathcal{B} & \dots & C\mathcal{A}^0\mathcal{B} & D \end{bmatrix} \\ \Phi^y &= \begin{bmatrix} C\mathcal{A}^0K \\ \vdots \\ C\mathcal{A}^{h-2}K & \dots & C\mathcal{A}^0K \end{bmatrix}. \end{aligned} \quad (22)$$

As expected from the state-space model (16),  $\Phi^p$  is an observability matrix and the Toeplitz matrices  $\Phi^u$  and  $\Phi^y$  contain the Markov parameters  $D, C\mathcal{A}^i\mathcal{B}$ , and  $C\mathcal{A}^iK$ .

Given  $\Phi^p$ ,  $\Phi^u$ , and  $\Phi^y$ , the state-space predictor matrices  $P_{\text{sts}}$  and  $F_{\text{sts}}$  can be formed according to (14). To quantify uncertainty, the one-step-ahead error covariance matrix estimate

$$(\tilde{Y}_1 - P_1\tilde{Z} - F_{11}\tilde{U}_1)(\tilde{Y}_1 - P_1\tilde{Z} - F_{11}\tilde{U}_1)^\top/n$$

or the trajectory error covariance matrix estimate

$$(\tilde{Y} - P\tilde{Z} - F\tilde{U})(\tilde{Y} - P\tilde{Z} - F\tilde{U})^\top/n$$

can be computed, optionally subtracting the number of estimated parameters,  $k = n_y(mn_z + n_u)$ , in the denominators.

Algorithm 2 summarizes the construction of the state-space predictor. Theorem 3 establishes its equivalence to the state-space model (16).

**Theorem 3.** Form  $A, B, C, D, K, P, F$ , and  $\Phi^y$  according to Algorithm 2 and let  $e_f(t) = (I - \Phi^y)^{-1}\varepsilon_f(t)$ . Then  $z_p(t)$ ,  $u_f(t) = (u(t), \dots, u(t+h-1))$ , and  $y_f(t) = (y(t), \dots, y(t+h-1))$  satisfy (3) if and only if

$$\begin{aligned} z_p(t+i+1) &= Az_p(t+i) + Bu(t+i) + K\varepsilon(t+i) \\ y(t+i) &= Cz_p(t+i) + Du(t+i) + \varepsilon(t+i) \end{aligned} \quad (23)$$

for  $i = 0, \dots, h-1$ .

*Proof.* For the ‘if’ direction, the preceding discussion showed that iteratively applying the state-space model (16) with any  $A, B, C, D$ , and  $K$  generates a trajectory predictor of the form (3) with  $P$  and  $F$  of the form (14) and  $\Phi^p, \Phi^u, \Phi^y$  of the form (22).

The ‘only if’ direction proceeds by induction. At  $i = 0$ , the first block row of  $e_f(t) = (I - \Phi^y)^{-1}\varepsilon_f(t)$  gives  $e(t) = \varepsilon(t)$ , so the result holds by Lemma 2. For the inductive step, we suppose that at some  $i$ , the result holds for  $j = 0, \dots, i-1$ . Under this assumption, iteratively applying (20) gives

$$z_p(t+i) = \mathcal{A}^i z_p(t) + \sum_{j=0}^{i-1} \mathcal{A}^{i-j-1} (\mathcal{B}u(t+j) + Ky(t+j)).$$

As  $P, F$ , and  $e_f(t)$  are constructed according to (14) and (22),  $y(t+i)$  satisfies (21). Comparing (21) to the expression above for  $z_p(t+i)$  shows that the output equation in (23) holds. With the output equation in hand, the same argument from the proof of Lemma 2 shows that the dynamics equation in (23) holds with  $A, B$ , and  $K$  defined as in (18).  $\blacksquare$

Theorem 3 implies that TPC with the state-space predictor is effectively a special case of MPC with the state-space model (16). More concretely, the TPC problem (4) is equivalent to the following MPC problem:

$$\begin{aligned} &\text{minimize} \quad c_0((u(1|t), \dots, u(h|t)), (y(1|t), \dots, y(h|t))) \\ &\text{subject to} \\ &c_j((u(1|t), \dots, u(h|t)), (y(1|t), \dots, y(h|t))) \leq 0, \\ &j = 1, \dots, J \\ &x(1|t) = z_p(t) \\ &x(i+1|t) = Ax(i|t) + Bu(i|t), \quad i = 1, \dots, h \\ &y(i|t) = Cx(i|t) + Du(i|t), \quad i = 1, \dots, h, \end{aligned} \quad (24)$$

with variables  $x(1|t), \dots, x(h+1|t), u(1|t), \dots, u(h|t), y(1|t), \dots, y(h|t)$  and with  $A, B, C$ , and  $D$  defined by (18). Corollary 4 formalizes this observation.

**Corollary 4.** Define  $A, B, C, D, P$ , and  $F$  as in Algorithm 2. Then

$$u_f^*(t) = \begin{bmatrix} u^*(1|t) \\ \vdots \\ u^*(h|t) \end{bmatrix}, \quad y_f^*(t) = \begin{bmatrix} y^*(1|t) \\ \vdots \\ y^*(h|t) \end{bmatrix}$$

are optimal for the TPC problem (4) if and only if  $u^*(1|t), \dots, u^*(h|t)$ ,  $y^*(1|t), \dots, y^*(h|t)$ , and  $x^*(1|t), \dots, x^*(h+1|t)$  are optimal for the MPC problem (24).

*Proof.* The result follows from Theorem 3, which establishes a bijection between the variables of (4) and (24).  $\blacksquare$

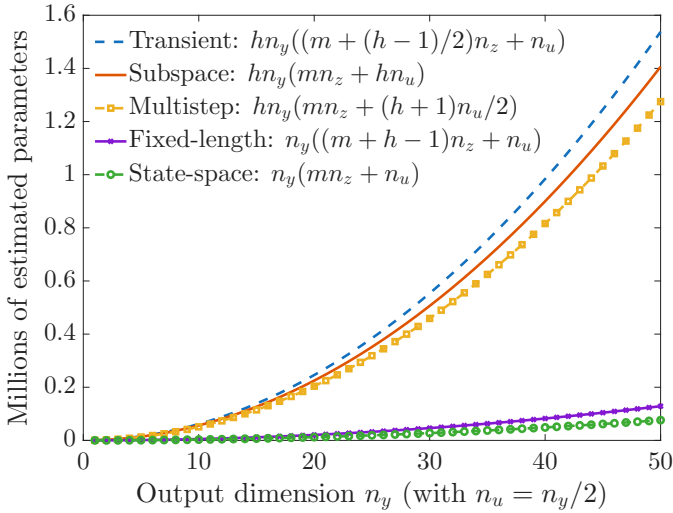


Fig. 1. Number of estimated parameters in each trajectory predictor. Formulas are general; curves use memory  $m = 20$ , prediction horizon  $h = 15$ , and input dimension  $n_u = n_y/2$ .

Unlike most output-feedback MPC methods, TPC with the state-space predictor does not require a state estimator. This is because the controller has perfect knowledge of the state  $z_p(t)$ , which is just the recent inputs  $u(t-m), \dots, u(t-1)$  interleaved with the recent outputs  $y(t-m), \dots, y(t-1)$ .

#### A. Trajectory predictor comparisons

The subspace predictor is the only trajectory predictor discussed above that is not causal. Numerical experiments suggest that it may perform poorly when training data are gathered in closed loop [32], [29], [30]. This may make the subspace predictor unsuitable for adaptive control, where the predictor is regularly updated using recent closed-loop data, and for applications where it is unsafe or impractical to excite the system with open-loop inputs to gather training data.

Different predictors require estimating different numbers of parameters. Fig. 1 shows how the number of estimated parameters in each predictor scales with the system dimensions. The formulas in the upper left are general; the curves are drawn for the example of  $m = 20$ ,  $h = 15$ , and  $n_u = n_y/2$ . The transient, subspace, and multistep predictors require estimating about an order of magnitude more parameters than the fixed-length and state-space predictors. The fixed-length and state-space predictors' favorable scaling may make them preferable for large-scale systems or for applications where it is costly or impractical to gather a large training dataset, as fitting models with more parameters generally requires more data. Because the state-space predictor only requires a one-step-ahead fit, it also makes slightly more efficient use of data, converting  $\tilde{z}(1), \dots, \tilde{z}(d)$  into  $d - m$  identification examples, compared to  $d - m - h + 1$  for the other predictors.

Fitting a trajectory predictor involves computing the pseudo-inverse of a data matrix. The data matrix must have full row rank for the pseudo-inverse to be well-defined in this context, so the data matrix must have at least as many columns as rows. This sets a minimum number of training examples required to fit the predictor. For example, the subspace and multistep

TABLE I  
MINIMUM NUMBER OF TRAINING EXAMPLES TO FIT EACH PREDICTOR

	Minimum # of examples	# less than transient
Transient	$(n_z + 1)(m + h) - n_y - 1$	
Subspace	$(n_z + 1)m + (n_u + 1)h - 1$	$(h - 1)n_y$
Multistep	$(n_z + 1)m + (n_u + 1)h - 1$	$(h - 1)n_y$
Fixed-length	$(n_z + 1)m + h + n_u - 1$	$(h - 1)n_z$
State-space	$(n_z + 1)m + n_u$	$(h - 1)(n_z + 1)$

predictors use a data matrix  $[\tilde{Z}^\top \quad \tilde{U}^\top]^\top$  with  $mn_z + hn_u$  rows and  $d - m - h + 1$  columns, so the number of training examples must satisfy  $d \geq (n_z + 1)m + (n_u + 1)h - 1$ . Table I shows the data requirements for the other predictors. The state-space predictor requires the fewest training examples. With  $h = 15$  and  $n_z = 10$ , for example, the state-space predictor can be fit to 154 fewer examples than the transient predictor.

Theorem 3 shows that the state-space predictor corresponds to the state-space model (16). This reduces TPC with the state-space predictor to a special case of MPC with an LTI state-space model. TPC with the state-space predictor therefore inherits the theoretical guarantees that linear MPC enjoys [17], such as conditions for stability [18] and recursive feasibility [19]. TPC with the state-space predictor can be extended to a robust [20], stochastic [21], or scenario [22] framework using established methods. The state-space predictor also enables control methods other than MPC, such as  $H_2$  or  $H_\infty$  optimal control, system-level synthesis [35], distributionally robust regret-optimal control [36], and so on.

## V. NUMERICAL EXPERIMENTS

To facilitate reproducibility and comparison with past results, we consider the double integrator example from [26], [29]. Moffat et al. Euler-discretize the continuous-time dynamics  $\dot{x}_1 = x_2 + w_1$ ,  $\dot{x}_2 = u + w_2$  with unit time step:

$$x(t+1) = \begin{bmatrix} 1 & 1 \\ 0 & 1 \end{bmatrix} x(t) + \begin{bmatrix} 0 \\ 1 \end{bmatrix} u(t) + w(t)$$

$$y(t) = x(t) + v(t).$$

All random variables are independent and (except the reference  $y_r(t)$ ) zero-mean Gaussian. The disturbance  $w(t)$  has covariance  $\text{diag}(0.0025, 0.0001)$ . The noise  $v(t)$  has covariance  $0.0004I_2$ . To gather open-loop training data, we use 0.01-variance noise for  $u(t)$ . To gather closed-loop training data, we use discrete proportional-derivative control,  $u(t) = -[0.0833 \quad 0.7944] (y(t) - y_r(t))$  plus 0.01-variance noise for additional excitation. The cost is the sum over  $t$  of

$$(y(t) - y_r(t))^\top \text{diag}(1000, 10)(y(t) - y_r(t)) + u(t)^2$$

with  $y_r(t) = (y_{r1}(t), 0)$ . We generate  $y_{r1}$  as a sequence of steps with uniform random durations on  $\{1, \dots, 50\}$  and magnitudes on  $[-5, 5]$ . There are no constraints beyond  $y_f(t) = Pz_p(t) + Fu_f(t)$  (in the  $r = \delta_0$  case), which allows elimination of  $y_f(t)$ . This reduces the TPC problem (4) to an unconstrained convex quadratic program with solution

$$u_f^*(t) = -(F^\top QF + I_{hn_u})^{-1} F^\top Q(Pz_p(t) - \hat{y}_{rf}(t)),$$

where  $Q = I_h \otimes \text{diag}(1000, 10)$ . For the predicted reference trajectory  $\hat{y}_{rf}(t) = (\hat{y}_r(t), \dots, \hat{y}_r(t+h-1)) \in \mathbf{R}^{hn_y}$ , we use the persistence model  $\hat{y}_r(t+i) = y_r(t-1)$  for all  $i$ .

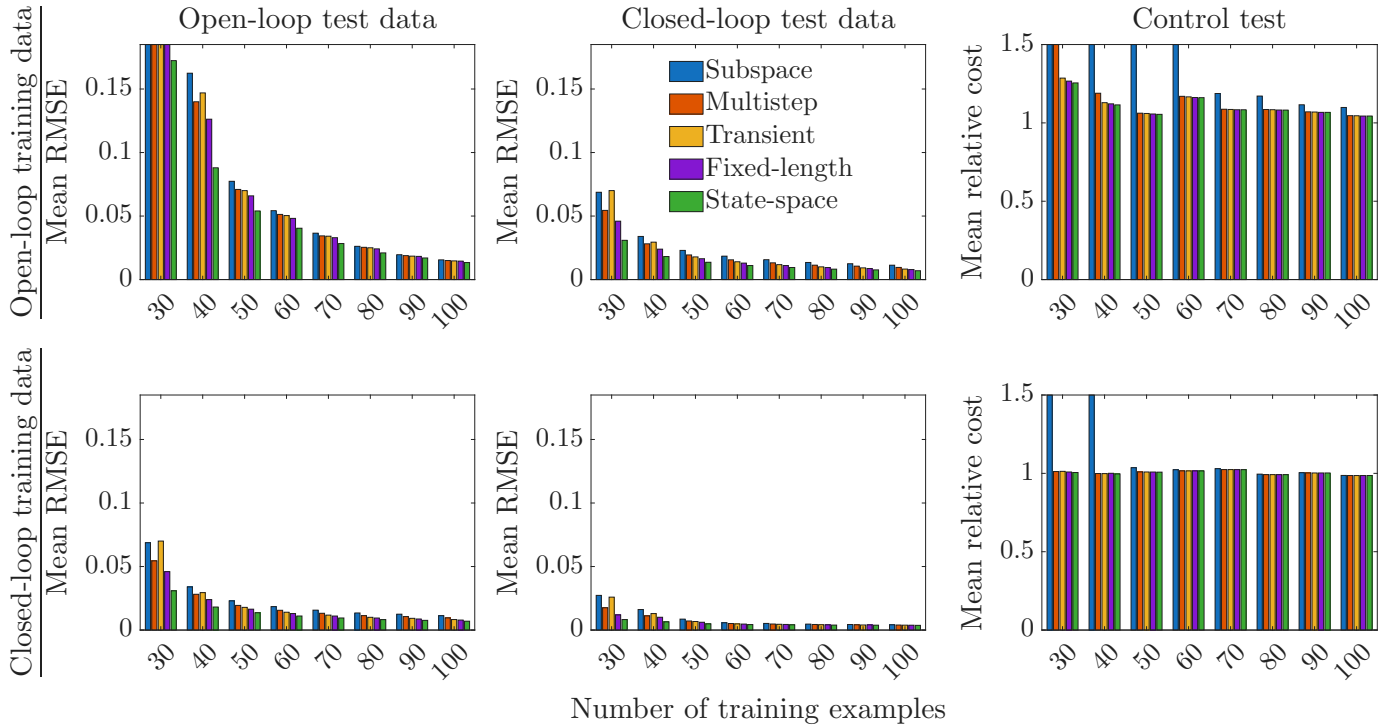


Fig. 2. Mean prediction RMSEs for each predictor on test data gathered in open (left column) and closed loop (center) with training data gathered in open (top row) and closed loop (bottom) over 1,000 Monte Carlo runs. Mean control costs (right) are normalized by the oracle LQG mean cost.

#### A. Predictor generalization and closed-loop performance

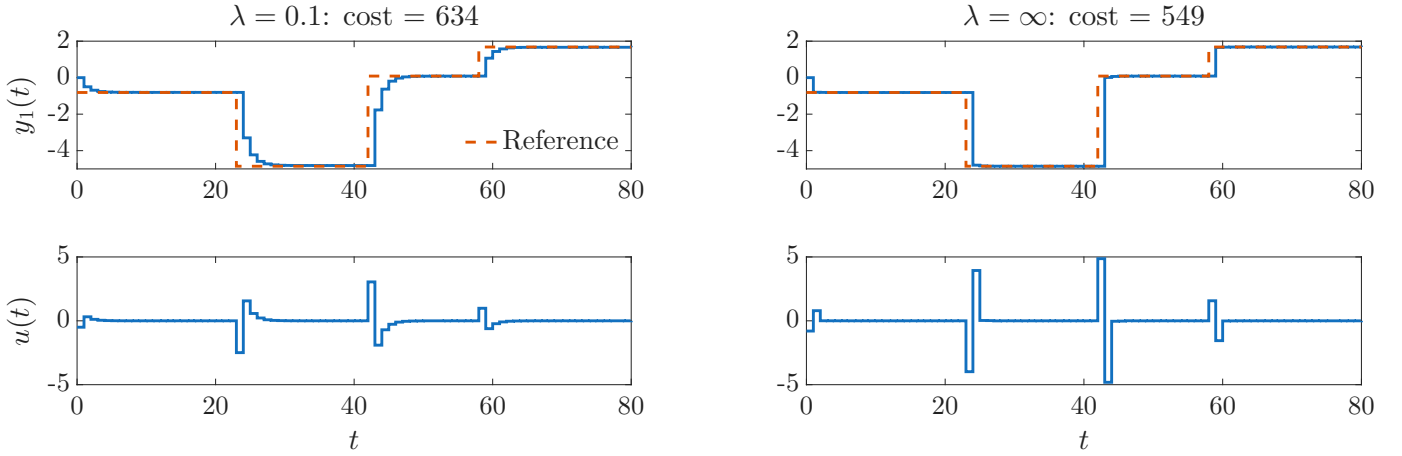
We evaluate TPC with the subspace, multistep, transient, fixed-length, and state-space predictors using Monte Carlo simulation. In each Monte Carlo run, we identify one version of each predictor from open-loop data and a second version from closed-loop data. For each predictor and training dataset, we select the memory  $m$  that minimizes the Akaike information criterion (AIC) [37], averaged over elements of  $y$  and over steps ahead in the prediction horizon. The AIC, an estimate of the information lost when representing the data-generating process by a given model, generally suggests longer memories for larger training datasets. For the predictors and training dataset sizes investigated here, the AIC usually suggests a memory of one or two time steps and rarely more than three. We test prediction accuracy for both versions of each predictor on two fresh datasets, again gathering one test dataset in open loop and one in closed loop. For control, we test TPC with both versions of each predictor on a fresh dataset, benchmarked against an oracle LQG controller that has perfect knowledge of the underlying system model. We use a prediction horizon of  $h = 10$  time steps for all predictors in all data configurations. With this horizon, TPC with all predictors performs well given sufficient training data.

Fig. 2 shows how prediction errors and control costs scale with the training dataset size  $d$  for each predictor. Bar heights are sample means over 1,000 Monte Carlo simulations with a test duration of 400 time steps. Training datasets are gathered in open loop for the top row of plots and closed loop for the bottom. The left and center columns show prediction root mean square errors (RMSEs) on test data gathered in open and closed loop, respectively. RMSEs are averaged over

elements of  $y$  and over steps-ahead predictors. In the top left plot, the  $d = 30$  bars for all predictors other than the state-space predictor extend well beyond the upper vertical axis limit, from 0.27 for the fixed-length predictor to 0.38 for the subspace predictor. As expected, test RMSEs decrease for all predictors as the training dataset size increases. All predictors have lower RMSEs predicting closed-loop test data, even if they are trained on open-loop data. Similarly, all predictors have lower RMSEs when trained on closed-loop data, even if they are predicting open-loop test data. Across all dataset sizes and data configurations, the subspace predictor has the highest RMSEs, the state-space predictor has the lowest, and the other three predictors are in between.

The righthand column in Fig. 2 shows the sample mean control cost (which penalizes both output tracking errors and control effort) for each predictor, normalized by the oracle LQG mean cost. For training data gathered in open loop (top), costs decrease as the training dataset grows. In this case, TPC with all predictors other than the subspace predictor is within 5% of the oracle LQG limit by  $d = 100$ . Perhaps surprisingly, costs for all predictors are systematically lower for training data gathered in closed loop (bottom). In this case, TPC with all predictors other than the subspace predictor is within 1% of the LQG limit by  $d = 30$ .

Fig. 2 shows that the least-structured predictor (the subspace predictor) consistently has the worst predictive accuracy and closed-loop performance. For small training datasets, TPC with the subspace predictor can be unstable, giving mean costs that exceed the upper vertical axis limit by many orders of magnitude. Prediction accuracy and closed-loop performance improve for predictors with more internal structure. The largest



**Fig. 3.** TPC output  $y_1$  (top row) and input  $u$  (bottom) with (left column) and without (right) relaxing the equality constraint in (4) and regularizing the slack variable  $e_f(t)$ . While the relax-and-regularize approach uses less control effort, it performs worse for tracking and worse overall.

improvement comes from imposing causal structure on the subspace predictor, which produces the multistep predictor. Imposing further structure, as in the transient, fixed-length, and state-space predictors, yields smaller improvements. The most structured predictor (the state-space predictor) has the fewest parameters and the best accuracy and closed-loop performance. Differences in predictive accuracy and closed-loop performance across predictors are largest for the smallest training datasets and tend to vanish as the training dataset grows. Based on these observations, we interpret structural constraints on the predictor as a form of implicit regularization that improves generalization by mitigating the risk of overfitting small training datasets.

### B. Relaxation and regularization

The examples in §V-A used the regularizer  $r = \delta_0$ , reducing the general TPC problem (2) to (4). This section explores relaxing the equality constraint in (4) by introducing the slack variable  $e_f(t)$  and augmenting the cost function with Tikhonov regularization, giving (2) with  $r(e_f(t)) = \lambda \|e_f(t)\|_2^2$ . Eliminating  $y_f(t)$  reduces (2) to an unconstrained convex quadratic program in  $(u_f(t), e_f(t))$  with solution satisfying

$$\begin{bmatrix} F^\top QF & F^\top Q \\ QF & Q + \lambda I \end{bmatrix} \begin{bmatrix} u_f^*(t) \\ e_f^*(t) \end{bmatrix} = \begin{bmatrix} F^\top \\ I \end{bmatrix} Q(Pz_p(t) - \hat{y}_{rf}(t)).$$

The matrix on the lefthand side is invertible if  $F$  has full column rank. We implement the ‘relax-and-regularize’ TPC policy with the state-space predictor identified from  $d = 50$  closed-loop training examples. The simulation setup is otherwise the same as in §V-A.

Fig. 3 shows the closed-loop output  $y_1$  (top row) and input  $u$  (bottom) for a TPC simulation with the relax-and-regularize approach and weight  $\lambda = 0.1$  (left column), and for TPC with  $r = \delta_0$  (right). The bottom plots show that the relax-and-regularize approach uses less control effort. However, it also leads to worse tracking performance, as shown by the slower step responses in the top left plot than in the top right plot. This is an example of optimism bias [26]: Relaxing the equality constraint allows the optimization to choose a

favorable realization of  $e_f(t)$  that would help steer the output toward the reference. In this sense, the relax-and-regularize approach can be viewed as conceptually opposite to the robust optimization approach, which would view  $e_f(t)$  as chosen adversarially and hedge against the worst-case realization. On average over 1,000 Monte Carlo runs with the setup described above, relaxing the equality constraint and regularizing  $e_f(t)$  increases the overall cost realized in closed loop by 14%.

## VI. LIMITATIONS AND FUTURE WORK

This paper defined TPC as a control framework that unifies a wide variety of indirect DDPC methods. This paper introduced the state-space predictor and showed that with it, TPC is a special case of MPC with an LTI state-space model. This result equips TPC – and with minor adjustments, most indirect DDPC methods of which the authors are aware – with linear MPC’s mature theory, including conditions for stability and recursive feasibility. In numerical experiments, TPC with a variety of predictors approached the performance limit of an oracle LQG controller with exact knowledge of the underlying system model. For all predictors, TPC performed better with closed-loop training data than with open-loop training data. TPC with the state-space predictor performed as well as TPC with any other predictor, and somewhat better than the others for small training datasets.

There are many opportunities to extend this work. Certificates of stability and recursive feasibility could be formalized by reducing TPC to MPC via the state-space predictor. Robust, stochastic, scenario, or adaptive TPC implementations could be developed similarly. The relax-and-regularize approach to TPC could be explored more deeply, particularly in the adaptive control setting, where connections might be made to optimistic exploration in reinforcement learning. TPC could be evaluated for time-varying or nonlinear systems and modified if necessary. Finally, TPC could be demonstrated in hardware and its deployment effort and closed-loop performance compared to existing methods.

## VII. ACKNOWLEDGMENTS

LDRP gratefully acknowledges support from the National Science Foundation's Graduate Research Fellowship Program. LDRP and AJK thank the American Society of Heating, Refrigeration, and Air-Conditioning Engineers (ASHRAE) for support from the Grant-In-Aid Award.

- [1] M. Morari and J. H. Lee, "Model predictive control: Past, present and future," *Computers & Chemical Engineering*, vol. 23, no. 4-5, pp. 667-682, 1999.
- [2] W. Favoreel, B. De Moor, and M. Gevers, "SPC: Subspace predictive control," *IFAC Proceedings Volumes*, vol. 32, no. 2, pp. 4004-4009, 1999.
- [3] J. Berberich and F. Allgöwer, "An overview of systems-theoretic guarantees in data-driven model predictive control," *Annual Review of Control, Robotics, and Autonomous Systems*, vol. 8, no. 1, pp. 77-100, 2025.
- [4] V. Krishnan and F. Pasqualetti, "On direct vs indirect data-driven predictive control," in *2021 60th IEEE Conference on Decision and Control (CDC)*. IEEE, 2021, pp. 736-741.
- [5] F. Dörfler, "Data-driven control: Part two of two: Hot take: Why not go with models?" *IEEE Control Systems Magazine*, vol. 43, no. 6, pp. 27-31, 2023.
- [6] J. Coulson, J. Lygeros, and F. Dörfler, "Data-enabled predictive control: In the shallows of the DeePC," in *2019 18th European Control Conference (ECC)*. IEEE, 2019, pp. 307-312.
- [7] J. C. Willems, "The behavioral approach to open and interconnected systems," *IEEE Control Systems Magazine*, vol. 27, no. 6, pp. 46-99, 2007.
- [8] I. Markovsky and F. Dörfler, "Behavioral systems theory in data-driven analysis, signal processing, and control," *Annual Reviews in Control*, vol. 52, pp. 42-64, 2021.
- [9] J. Berberich, J. Köhler, M. A. Müller, and F. Allgöwer, "Data-driven model predictive control with stability and robustness guarantees," *IEEE Transactions on Automatic Control*, vol. 66, no. 4, pp. 1702-1717, 2020.
- [10] J. Coulson, J. Lygeros, and F. Dörfler, "Distributionally robust chance constrained data-enabled predictive control," *IEEE Transactions on Automatic Control*, vol. 67, no. 7, pp. 3289-3304, 2021.
- [11] F. Dörfler, J. Coulson, and I. Markovsky, "Bridging direct and indirect data-driven control formulations via regularizations and relaxations," *IEEE Transactions on Automatic Control*, vol. 68, no. 2, pp. 883-897, 2022.
- [12] L. Huang, J. Zhen, J. Lygeros, and F. Dörfler, "Robust data-enabled predictive control: Tractable formulations and performance guarantees," *IEEE Transactions on Automatic Control*, vol. 68, no. 5, pp. 3163-3170, 2023.
- [13] V. Breschi, A. Chiuso, and S. Formentin, "Data-driven predictive control in a stochastic setting: A unified framework," *Automatica*, vol. 152, p. 110961, 2023.
- [14] A. Chiuso, M. Fabris, V. Breschi, and S. Formentin, "Harnessing uncertainty for a separation principle in direct data-driven predictive control," *Automatica*, vol. 173, p. 112070, 2025.
- [15] P. Van Overschee and B. De Moor, "N4SID: Subspace algorithms for the identification of combined deterministic-stochastic systems," *Automatica*, vol. 30, no. 1, pp. 75-93, 1994.
- [16] M. Verhaegen and P. Dewilde, "Subspace model identification part 2: Analysis of the elementary output-error state-space model identification algorithm," *International Journal of Control*, vol. 56, no. 5, pp. 1211-1241, 1992.
- [17] J. B. Rawlings, D. Q. Mayne, M. Diehl *et al.*, *Model predictive control: Theory, computation, and design*. Nob Hill Publishing Madison, WI, 2020, vol. 2.
- [18] D. Q. Mayne, J. B. Rawlings, C. V. Rao, and P. O. Scokaert, "Constrained model predictive control: Stability and optimality," *Automatica*, vol. 36, no. 6, pp. 789-814, 2000.
- [19] J. Löfberg, "Oops! I cannot do it again: Testing for recursive feasibility in MPC," *Automatica*, vol. 48, no. 3, pp. 550-555, 2012.
- [20] A. Bemporad and M. Morari, "Robust model predictive control: A survey," in *Robustness in Identification and Control*. Springer, 2007, pp. 207-226.
- [21] A. Mesbah, "Stochastic model predictive control: An overview and perspectives for future research," *IEEE Control Systems Magazine*, vol. 36, no. 6, pp. 30-44, 2016.
- [22] G. C. Calafiore and L. Fagiano, "Robust model predictive control via scenario optimization," *IEEE Transactions on Automatic Control*, vol. 58, no. 1, pp. 219-224, 2012.
- [23] S. Boyd and L. Vandenberghe, *Convex optimization*. Cambridge University Press, 2004.
- [24] J. C. Willems, P. Rapisarda, I. Markovsky, and B. L. De Moor, "A note on persistency of excitation," *Systems & Control Letters*, vol. 54, no. 4, pp. 325-329, 2005.
- [25] I. Markovsky, E. Prieto-Araujo, and F. Dörfler, "On the persistency of excitation," *Automatica*, vol. 147, p. 110657, 2023.
- [26] K. Moffat, F. Dörfler, and A. Chiuso, "The bias of subspace-based data-driven predictive control," *arXiv preprint arXiv:2507.02468*, 2025.
- [27] R. Dinkla, S. P. Mulders, J.-W. van Wingerden, and T. Oomen, "Closed-loop aspects of data-enabled predictive control," *IFAC-PapersOnLine*, vol. 56, no. 2, pp. 1388-1393, 2023.
- [28] J. Coulson, J. Lygeros, and F. Dörfler, "Regularized and distributionally robust data-enabled predictive control," in *2019 IEEE 58th Conference on Decision and Control (CDC)*. IEEE, 2019, pp. 2696-2701.
- [29] K. Moffat, F. Dörfler, and A. Chiuso, "The transient predictor," in *2024 IEEE 63rd Conference on Decision and Control (CDC)*. IEEE, 2024, pp. 1871-1876.
- [30] M. Sader, Y. Wang, D. Huang, C. Shang, and B. Huang, "Causality-informed data-driven predictive control," *IEEE Transactions on Control Systems Technology*, 2025.
- [31] D. S. Bernstein, *Matrix mathematics: Theory, facts, and formulas*. Princeton University Press, 2009.
- [32] J. Dong, M. Verhaegen, and E. Holweg, "Closed-loop subspace predictive control for fault tolerant MPC design," *IFAC Proceedings Volumes*, vol. 41, no. 2, pp. 3216-3221, 2008.
- [33] A. Liu and M. Jansson, "Closed-loop consistent, causal data-driven predictive control via SSARX," *arXiv preprint arXiv:2512.14510*, 2025.
- [34] M. Jansson, "Subspace identification and ARX modeling," *IFAC Proceedings Volumes*, vol. 36, no. 16, pp. 1585-1590, 2003.
- [35] J. Anderson, J. C. Doyle, S. H. Low, and N. Matni, "System level synthesis," *Annual Reviews in Control*, vol. 47, pp. 364-393, 2019.
- [36] F. Al Taha, S. Yan, and E. Bitar, "A distributionally robust approach to regret optimal control using the Wasserstein distance," in *2023 62nd IEEE Conference on Decision and Control (CDC)*. IEEE, 2023, pp. 2768-2775.
- [37] H. Akaike, "A new look at the statistical model identification," *IEEE Transactions on Automatic Control*, vol. 19, no. 6, pp. 716-723, 1974.